BRAIN COMMUNICATIONS

Accelerated decline in white matter microstructure in subsequently impaired older adults and its relationship with cognitive decline

Andrea T. Shafer,[1]* Owen A. Williams,[1,2]* Evian Perez,[3] Yang An,[1] Bennett A. Landman,[4] Luigi Ferrucci[5] and Susan M. Resnick[1]

* Joint first authors.

Little is known about a longitudinal decline in white matter microstructure and its associations with cognition in preclinical dementia. Longitudinal diffusion tensor imaging and neuropsychological testing were performed in 50 older adults who subsequently developed mild cognitive impairment or dementia (subsequently impaired) and 200 cognitively normal controls. Rates of white matter microstructural decline were compared between groups using voxel-wise linear mixed-effects models. Associations between change in white matter microstructure and cognition were examined. Subsequently impaired individuals had a faster decline in fractional anisotropy in the right inferior fronto-occipital fasciculus and bilateral splenium of the corpus callosum. A decline in right inferior fronto-occipital fasciculus fractional anisotropy was related to a decline in verbal memory, visuospatial ability, processing speed and mini-mental state examination. A decline in bilateral splenium fractional anisotropy was related to a decline in verbal fluency, processing speed and mini-mental state examination. Accelerated regional white matter microstructural decline is evident during the preclinical phase of mild cognitive impairment/dementia and is related to domain-specific cognitive decline.

1 Laboratory of Behavioral Neuroscience, National Institute on Aging, Baltimore, MD 21224, USA
2 Department of Experimental Psychology, University of Oxford, Oxford, UK
3 San Juan Bautista School of Medicine, Caguas, Puerto Rico
4 School of Engineering, Vanderbilt University, Nashville, TN, USA
5 Longitudinal Studies Section, Translational Gerontology Branch, National Institute on Aging, Baltimore, MD 21224, USA

Correspondence to: Andrea T. Shafer
251 Bayview Blvd., Baltimore
MD 21224, USA
E-mail: andrea.shafer@nih.gov

Correspondence may also be addressed to: Susan M. Resnick
E-mail: resnicks@grc.nia.nih.gov

Keywords: diffusion tensor imaging; preclinical Alzheimer's disease; longitudinal change; white matter microstructure; cognition

Abbreviations: 3 T = 3 Tesla; APOE = apolipoprotein E; Aβ = beta-amyloid; BIMC = Blessed Information-Memory-Concentration; BLSA = Baltimore Longitudinal Study of Aging; CDR = Clinical Dementia Rating; CN = cognitively normal; DTI = diffusion tensor imaging; EOAD = early-onset Alzheimer's disease; FA = fractional anisotropy; FDR = false discovery rate; FLAIR = fluid-attenuated inversion recovery; IFOF = inferior fronto-occipital fasciculus; LME = linear mixed-effect; MCI = mild cognitive impairment; MD = mean diffusivity; MMSE = mini-mental state examination; MPRAGE = magnetization prepared rapid radient echo; MUSE = multi-atlas region segmentation utilizing ensembles; SCC = splenium of the corpus callosum; SD = standard deviation; SI = subsequently impaired; TBSS = tract-based spatial statistics; TE = echo time; TR = repetition time; WM = white matter; WMH = white matter hyperintensities

Received August 24, 2021. Revised January 03, 2022. Accepted February 25, 2022. Advance access publication March 1, 2022

Graphical Abstract

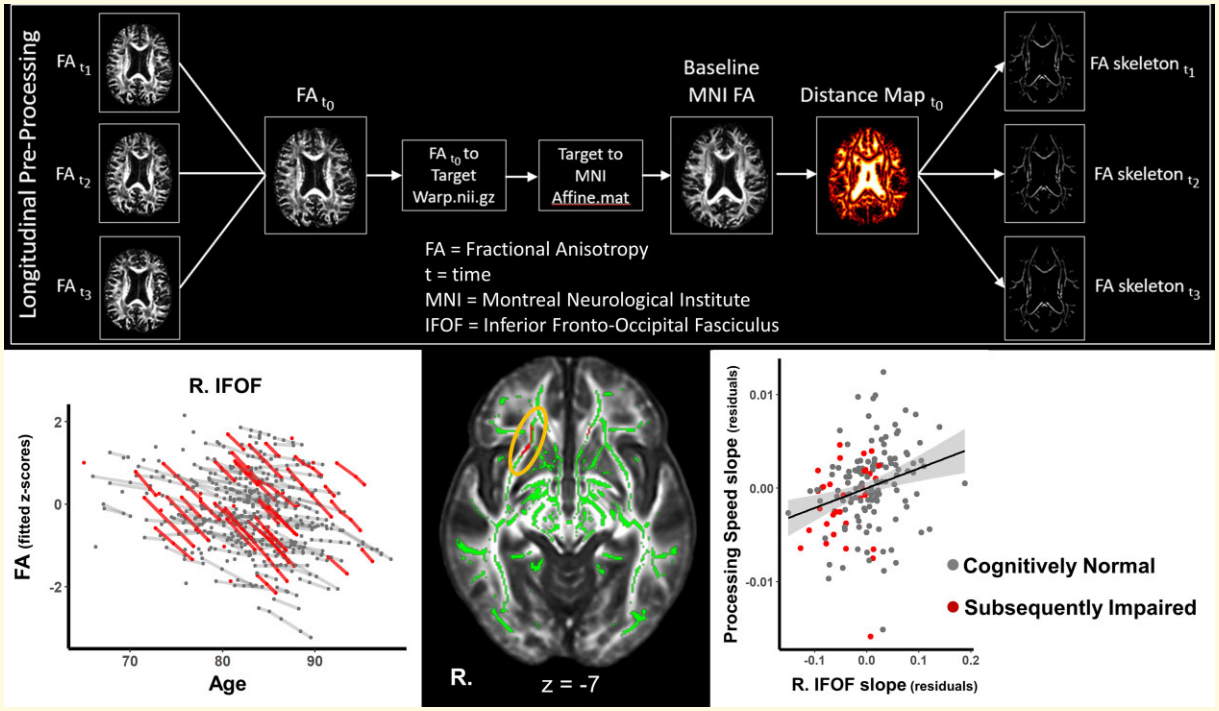

Introduction

Dementia is one of the leading causes of death and disability worldwide, and it is projected to affect over 151 million individuals by 2050.[1] Alzheimer's disease is the most common cause of dementia. Alzheimer's disease is a progressive neurodegenerative disease with a long preclinical phase typically defined by the accumulation of beta-amyloid (Aβ) and phosphorylated tau with a subsequent acceleration of regional brain atrophy in the absence of clinical symptoms.[2–5] However, the nature of longitudinal changes in white matter (WM) microstructure in the preclinical phase of Alzheimer's disease and other forms of dementia has been less well characterized.

Network-based research on Alzheimer's disease points to patterns of disconnection of spatially dispersed but functionally connected regions of the brain, e.g. the default mode network.[6,7] Functional networks are supported by the cerebral WM connecting the grey matter regions implicated in dementia. It is therefore important to understand the spatial pattern of structural alterations of WM in the preclinical stages of dementia. Diffusion tensor imaging (DTI) is an imaging technique that is sensitive to the microstructural properties of cerebral WM.[8] In the WM, axons, myelin sheaths and neurofilaments restrict both direction and magnitude of Brownian diffusion, leading to highly directional diffusion moving in parallel with WM tracts. Fractional anisotropy (FA) is used to quantify the degree of anisotropic diffusion and mean diffusivity (MD) is used to quantify the magnitude of total water diffusion within brain tissue.

Age-related decreases in FA and increases in MD have been widely reported from both cross-sectional and longitudinal studies and are thought to reflect microstructural damage that is associated with cognitive decline.[9–13] However, while preclinical dementia is associated with declines in several cognitive domains including episodic memory, executive functioning, visuospatial functioning and processing speed,[14,15] few studies have examined the associations between changes in DTI metrics and changes in cognition in preclinical dementia.[16]

DTI metrics have been shown to be a promising tool in detecting microstructural changes related to cognitive impairment and dementia, and in predicting subsequent dementia. Compromised WM microstructure (lower FA, higher MD) in Alzheimer's disease when compared to cognitively normal (CN) controls has been reported in the fornix, splenium of the corpus callosum (SCC), inferior fronto-occipital fasciculus (IFOF), and uncinate fasciculus.[17–19] Furthermore, global values of FA and MD acquired in a large sample without dementia were related to an increased risk in subsequent all-cause dementia and Alzheimer's disease.[20] When looking at the tract-level, lower FA in association tracts including the IFOF, uncinate fasciculus and limbic tracts (parahippocampal part of the cingulum and the fornix) was related to the risk of incident dementia.[20] However, longitudinal studies of alterations in WM microstructure during the preclinical phase are needed to fully understand the role of WM microstructural changes in the development of cognitive impairment and dementia.

Such studies are also critical to identify possible novel biomarkers for clinical trials with an increased focus on the asymptomatic preclinical stage of Alzheimer's disease, with the hope that interventions administered before neuronal damage and symptom onset may be more effective.[21,22]

The aim of the present study was to characterize the longitudinal trajectories of microstructural WM changes in preclinical mild cognitive impairment (MCI)/dementia and to interrogate their relationship with cognitive decline. To elucidate dementia-related regional changes in WM microstructure prior to symptom onset, we investigated voxel-wise differences in changes in FA and MD in individuals who later developed MCI or dementia versus those who remained CN. We hypothesized that observed differences in rates of microstructural change would be identified in regions previously implicated in dementia such as the cingulum, corpus callosum and medial temporal lobe WM. Furthermore, we assessed the associations between localized rates of change in DTI metrics and rates of change in cognition in domains that show a decline in the preclinical phase of MCI/dementia.

Materials and methods

Participants

Participants were from the Baltimore Longitudinal Study of Aging (BLSA), a prospective study of physical and psychological aging that started in 1958.[23] Participants were healthy at enrolment and those who were diagnosed over time with either MCI ($n = 30$) or dementia ($n = 20$) were matched based on baseline age, sex, race and follow-up time from first DTI, in a 1:4 ratio with participants with normal cognitive status throughout follow-up (MatchIt[24]), see Supplementary material and Supplementary Fig. 3 for more information. The BLSA study is approved by the Local Institutional Review Boards, and participants provided written informed consent at each visit.

The BLSA population used in the present study consists of community-dwelling volunteers 50 years of age and older who participated in the neuroimaging substudy[25] with concurrent neuropsychological testing and MRI data collected from 2009 to 2018. The BLSA visit schedules have varied over time depending on the age of the participant and over the course of the present study are as follows: BLSA participants aged younger than 60 years are assessed every 4 years; those aged 60–79 years are seen biennially, while BLSA participants ≥80 years are seen annually. Baseline was defined as the first DTI. For this study, participants were also free of significant health conditions that could substantially affect brain structure (i.e. closed head injury, brain surgery, malignant cancer, meningiomas and cysts with brain tissue displacement, seizure and bipolar disorders). If participants developed these conditions during the follow-up interval; any visits after the onset of a condition were removed.

Determination of cognitive status was performed through established procedures. Clinical and neuropsychological data from participants were reviewed at a consensus diagnostic case conference if their combined Clinical Dementia Rating (CDR) score[26] was ≥0.5 or if they had >3 errors on the Blessed Information-Memory-Concentration Test (BIMC[27]). The CDR was administered at 1–2-year intervals in certain BLSA substudies and to all participants scoring more than three errors on the BIMC. Diagnoses of dementia and Alzheimer's disease, respectively, were based on criteria outlined in the Diagnostic and Statistical Manual of Mental Disorders, third edition, revised[28] and the National Institute of Neurological and Communication Disorders and Stroke—Alzheimer's Disease and Related Disorders.[29] MCI was based on the Petersen criteria.[30]

Table 1 Participant characteristics stratified by cognitive groups

	Cognitively normal	Subsequently impaired	*P*-value
N	200	50	—
Age, mean (SD)	80.68 (5.30)	81.90 (6.26)	0.163
Sex (males %)	113 (56.5)	31 (62.0)	0.587
Race (Whites %)	153 (76.5)	41 (82.0)	0.519
Education, mean (SD)	16.94 (2.59)	17.10 (2.96)	0.728
APOE ε4 (%) [# missing]	37 (18.9) [4]	10 (20.8) [2]	0.917
Hypertension (%)	76 (39.2)	20 (40.8)	0.963
Elevated cholesterol (%)	57 (28.5)	13 (27.1)	0.986
Diabetes (%)	14 (7.3)	4 (8.7)	0.494
Obese (%)	30 (15.0)	5 (10.0)	0.494
White matter lesion volume cm^3, mean (SD)[a]	796.9 (1046.4)	791.9 (887.3)	0.974
Has longitudinal DTI (%)	135 (67.5)	33 (66.0)	0.973
Number of visits, *n* (%)			
1	200 (100.0)	50 (100.0)	
2	135 (67.5)	33 (66.0)	
3	86 (43.0)	17 (34.0)	
4	46 (23.0)	10 (20.0)	
5	17 (8.5)	3 (6.0)	
6	3 (1.5)	1 (2.0)	
Total number of longitudinal datapoints	422	97	
Follow-up, mean years (SD)	3.38 (1.51)	3.05 (1.32)	0.381
Baseline cognitive function, mean z-score (SD)			
Verbal memory	0.006 (0.928)	−0.046 (1.095)	0.766
Executive function	0.032 (0.785)	−0.158 (0.878)	0.183
Attention	−0.004 (0.775)	0.012 (0.681)	0.889
Verbal fluency	0.064 (0.829)	−0.237 (0.873)	0.031
Visuospatial ability	0.015 (0.987)	−0.061 (0.987)	0.64
Processing speed	0.061 (1.021)	−0.174 (0.87)	0.12
MMSE	0.011 (1.042)	−0.061 (0.829)	0.604
Time between last DTI and symptom onset, mean years (SD)	—	2.23 (1.28)	—

P-values were obtained from Welch's *t*-tests for continuous variables and χ^2-tests for categorical variables.
[a]White matter lesion data were unavailable for nine participants (five CN and four SI).

Table 1 provides the sample characteristics for both cognitive status groups [50 subsequently impaired (SI) and 200 CN participants]. For the SI group, the last DTI scan included in the analysis preceded the date of symptom onset. There were no significant differences between cognitive groups for any of the matching criteria including baseline age, sex, race and length of follow-up from the first 3T DTI scan. There were also no significant differences in years of education, apolipoprotein E (APOE) ε4 status, baseline WM lesion volume, and vascular risk factors including hypertension, elevated cholesterol, diabetes mellitus or obesity.

DTI acquisition and preprocessing

MRI data were acquired on three different 3 Tesla (3T) Philips Achieva scanners (Scanners 1 and 2 at the Kennedy Krieger Institute and Scanner 3 at the National Institute on Aging). The DTI acquisition was identical for Scanners 1 and 2 but was different for Scanner 3: DTI acquisition, Scanners 1 and 2: number of gradients = 32, number of *b*0 images = 1, max *b*-factor = 700 s/mm^2, repetition time (TR)/echo time (TE) = 6801/75 ms, number of slices = 65, voxel size = 0.83 mm × 0.83 mm × 2.2 mm, reconstruction matrix = 256 × 256, acquisition matrix = 96 × 95, field of view = 212 × 212 mm, flip angle = 90°. DTI acquisition, Scanner 3: number of gradients = 32, number of *b*0 images = 1, max *b*-factor = 700 s/mm^2, TR/TE = 7454/75 ms, number of slices = 70, voxel size = 0.81 mm × 0.81 mm × 2.2 mm, reconstruction matrix = 320 × 320, acquisition matrix = 116 × 115, field of view = 260 × 260 mm and flip angle = 90°. For all scanners, two separate DTI scans were acquired for each participant and subsequently combined to generate images with a number of signal averages = 2 to improve the signal to noise ratio.[31] Previous work has examined the reliability of diffusion measures across scanners in the BLSA and found acceptable levels of test–retest reliability.[32]

A general overview of the preprocessing steps is provided here, with more detailed information provided in the Supplementary material. DTI data were corrected for physiological motion effects and eddy currents. Tensor fitting was carried out using FMRIB Software Library FMRIB's Diffusion Toolbox using the ordinary least squares method. Resultant FA and MD maps were selected for analysis. Quality control methods for DTI data in the BLSA have been described previously.[31,33] Baseline motion and motion over time did not differ between groups, see Supplementary material.

The tract-based spatial statistics (TBSS[34]) analysis utilized a BLSA-specific FA template that was generated using advanced normalization tools MultivariateTemplateConstruction2[35] and FA images from 60 (30 men, 30 women) CN BLSA participants with a mean age of 69.9 years (range: 60–80 years). TBSS was used to generate a WM skeleton to facilitate voxel-wise analysis in WM tracts common to all participants. See Supplementary Fig. 1 for details of the processing pipeline.

WM lesion volumes

To ensure no group differences were present at baseline in cerebral small vessel disease that could influence the results, we performed a non-parametric *t*-test on total white matter hyperintensities (WMHs) volume. There were no group differences at baseline (see Table 1). Magnetization prepared rapid radient echo (MPRAGE) (TR = 6.8 ms, TE = 3.2 ms, flip angle = 8°, image matrix = 256 × 256 × 170, voxel size = 1 mm × 1 mm × 1.2 mm) and fluid-attenuated inversion recovery (FLAIR) (TR = 11 s, TE = 68 ms, inversion time = 2800 ms, image matrix = 240 × 240 × 150, voxel size = 0.83 mm × 0.83 mm × 3 mm) scans were acquired on a 3 T Philips Achieva scanners. MPRAGE scans were used to compute anatomical labels and regional brain volumes with multi-atlas region segmentation using an ensemble (MUSE) of registration algorithms and parameters[36]. FLAIR scans in conjunction with the MUSE segmented MPRAGE were then used with a convolutional deep neural network (DeepMRSeg) to segment the WM lesion volumes.[37]

Cognitive measures and domains

Composite scores were calculated for verbal memory, executive function, attention, visuospatial ability, verbal fluency and processing speed. The BLSA neuropsychological test battery has been described previously,[33,38] and details are provided in Supplementary Table 1. We also examined performance on a widely used, easy-to-implement assessment of general mental status and cognitive impairment, the mini-mental state examination (MMSE).[39] Cognitive domains were determined using theoretical constructs based on neuropsychological literature. This approach has been implemented in many prior studies utilizing the BLSA data.[40–42]

Statistical analyses

Differences in longitudinal WM microstructural trajectories due to subsequent impairment

Voxel-wise analysis was performed in MATLAB (Natick, Massachusetts: The MathWorks Inc.). To estimate group differences in longitudinal change in WM microstructure, linear mixed-effects (LME) models were implemented using fitlme (https://www.mathworks.com/help/stats/fitlme.html) with FA or MD as the dependent variable. The analysis was restricted to voxels in the mean FA skeleton image. Intercept and time (follow-up time in years from the first 3T DTI scan) were entered as random effects with unstructured covariance. Fixed effects included cognitive group (SI/preclinical = 1, cognitively stable = 0), mean-centered baseline age and sex, race, scanner, baseline motion (mean FD), and two-way interactions of cognitive group, baseline age, sex, and race with time, see Eq. (1). To control for the effect of multiple comparisons, contrasts of interest (the main effect of cognitive group and cognitive group × time interaction) were examined using a *P*-value of <0.005 and

cluster size of 30 voxels or more and also using a more conservative correction approach, false discovery rate (FDR).[43] For each cluster that met these requirements, the coordinates of the peak voxel (defined as highest *t*-value) were used to define the location of the cluster by comparison with the Johns Hopkins University International Consortium for Brain Mapping-DTI-81 WM labels atlas.[44] While the primary focus of this study was to assess group differences in *longitudinal* change in DTI metrics, we also report baseline results in Supplementary material.

$$\begin{aligned}\mathrm{FA}_{ij}/\mathrm{MD}_{ij} = {} & \beta_{0i} + \beta_1 \times \mathrm{Age}_i + \beta_2 \times \mathrm{Sex}_i + \beta_3 \times \mathrm{Race}_i \\ & + \beta_4 \times \mathrm{Cognitive\ Group}_i + \beta_5 \times \mathrm{Motion}_i \\ & + \beta_6 \times \mathrm{Scanner}_i + \beta_7 \times \mathrm{Time}_{ij} + \beta_8 \\ & \times (\mathrm{Age}_i \times \mathrm{Time}_{ij}) + \beta_9 \times (\mathrm{Sex}_i \times \mathrm{Time}_{ij}) \\ & + \beta_{10} \times (\mathrm{Race}_i \times \mathrm{Time}_{ij}) + \beta_{11} \\ & \times (\mathrm{Cognitive\ Group}_i \times \mathrm{Time}_{ij}) + e_{ij} \qquad (1)\end{aligned}$$

Relationship between change in FA and change in cognition

We first used LME models to examine cognitive change in the SI relative to the CN group. The same LME models were used to estimate group differences in longitudinal change in cognition as were used for the DTI data, minus the fixed effects for scanner and baseline motion (R 3.3.2, nlme 3.1-139), see Eq. (2). Next, we assessed the amount of between-person variability in preclinical longitudinal change explained by the effect of interest (subsequent cognitive group) for each outcome (cognition and DTI). The amount of variance explained (R^2) in the change trajectory accounted for by the cognitive group is a measure of effect size used in multilevel models[45,46] and can provide an estimate of how sensitive the outcome is in detecting differences in change over time due to preclinical disease, see Supplementary material for additional information.

$$\begin{aligned}\mathrm{Cognition}_{ij} = {} & \beta_{0i} + \beta_1 \times \mathrm{Age}_i + \beta_2 \times \mathrm{Sex}_i + \beta_3 \times \mathrm{Race}_i \\ & + \beta_4 \times \mathrm{Cognitive\ Group}_i + \beta_5 \times \mathrm{Time}_{ij} + \beta_6 \\ & \times (\mathrm{Age}_i \times \mathrm{Time}_{ij}) + \beta_7 \times (\mathrm{Sex}_i \times \mathrm{Time}_{ij}) + \beta_8 \\ & \times (\mathrm{Race}_i \times \mathrm{Time}_{ij}) + \beta_9 \times (\mathrm{Cognitive\ Group}_i \\ & \times \mathrm{Time}_{ij}) + e_{ij} \qquad (2)\end{aligned}$$

Finally, we examined the relationship between change in FA and change in cognition, focusing on the three larger uncorrected FA clusters that survived FDR correction. To implement an unbiased slope estimates for FA and cognition, we performed simple LME models with intercept and time entered as random effects with unstructured covariance. Then, partial correlations controlling for age, sex, and race were used to assess the relationship between change in mean FA from each cluster and change in cognition. Partial correlations were performed using R and pcor.test.[47]

Data availability

Data from the BLSA are available on request from the BLSA website (http://blsa.nih.gov). All requests are reviewed by the BLSA Data Sharing Proposal Review Committee and may also be subject to approval from the National Institutes of Health institutional review board.

Results

Faster rates of WM microstructural change in the splenium and IFOF in those with subsequent impairment

The cognitive group × time interaction revealed 10 clusters where FA declined at faster rates over time in the SI group compared with the CN group (Table 2). The largest areas of decline were in the SCC and in the IFOF, see Fig. 1. Clusters in these areas survived FDR correction for multiple comparisons, but this correction resulted in smaller, separate clusters. For example, the largest cluster (right SCC, 728 voxels) became three smaller clusters of 124 voxels, 107 voxels and 67 voxels (Table 2). Other areas showing faster declines in FA were the superior cerebellar peduncle, postcentral gyrus WM, middle/lateral occipital gyrus WM, cingulate gyrus WM, genu of the corpus callosum and posterior corona radiata. However, these clusters did not survive FDR correction.

Six clusters were found to show faster increases in MD over time for the SI relative to the CN group and two clusters showed faster increases in MD in the CN versus SI group (Table 2). Of the six clusters showing a faster increase in MD for the SI group, four were in the SCC and the remaining two clusters were in the R. postcentral gyrus and L. posterior thalamic radiation. The two clusters with faster increases in MD in the CN group relative to the SI group were in the R. posterior thalamic radiation and R. cerebellar WM. None of the clusters showing a longitudinal change in MD survived FDR correction.

Correlations between change in FA and change in cognition

LME models controlling for age, sex, and race were performed to cognitively characterize this DTI subsample of the BLSA. Significantly faster rates of cognitive decline in SI compared with CN participants were observed for memory, executive function and processing speed (see Table 3 and Supplementary Fig. 2 and Table 3), but not for spatial ability or attention. Effect sizes for the group differences in rates of longitudinal change were estimated using an R^2 statistic for multilevel models in which the amount of residual variance in between-person slopes captured by cognitive status was calculated for cognitive and DTI measures. These showed that the cognitive status grouping explained more between-person variation in the longitudinal trajectories of FA (L.SCC, 76%; R. SCC, 84%; right IFOF, 61%) when compared with the

Table 2 White matter clusters showing differences in the rates of change in FA and MD between SI and CN groups

FA	Voxels	*t*-value	*X*	*Y*	*Z*	FDR[a]
Splenium corpus callosum (R)	728[b]	−5.34	21	−49	13	124, 107, 67
Splenium corpus callosum (L)	570[b]	−5.69	−24	−58	14	118, 58, 53
Inferior fronto-occipital fasciculus (R)	161[b]	−5.77	25	20	−7	42
Superior cerebellar peduncle (L)	55	−4.87	−7	−40	−26	
Postcentral gyrus WM (R)	48	−4.60	30	−18	48	
Postcentral gyrus WM (L)	47	−4.14	−24	−22	50	
Middle/lateral occipital gyrus WM (L)	37	−4.44	−29	−79	−2	
Cingulate gyrus WM (L)	31	−5.45	−10	−49	19	
Genu corpus callosum (L)	31	−4.63	−9	31	−3	
Posterior corona radiata (R)	30	−5.34	20	−52	27	
MD	**Voxels**	***t*-value**	***X***	***Y***	***Z***	**FDR[a]**
Splenium corpus callosum (R)	260	5.31	17	−45	15	
Splenium corpus callosum (L)	133	4.36	−15	−44	23	
Postcentral gyrus WM (R)	53	5.52	30	−17	46	
Splenium corpus callosum (L)	43	4.62	−7	−34	25	
Posterior thalamic radiation (L)	38	4.40	−28	−60	14	
Posterior thalamic radiation (R)	38	−3.71	34	−36	14	
Splenium corpus callosum (R)	35	3.57	15	−36	29	
Cerebellar WM (R)	32	−3.55	23	−64	−48	

The peak *t*-value is reported for each cluster. FA, fractional anisotropy; MD, mean diffusivity; R, right, L, left; FDR, false discovery rate correction; SI, subsequently impaired; CN, cognitively normal.

[a]Effects that survived FDR correction were split into smaller clusters. Values represent the number of voxels in FDR clusters. Peak coordinates are from the BLSA FA template affine aligned to MNI space. Analysis $n = 250$.

[b]Clusters extracted for brain–behaviour correlations.

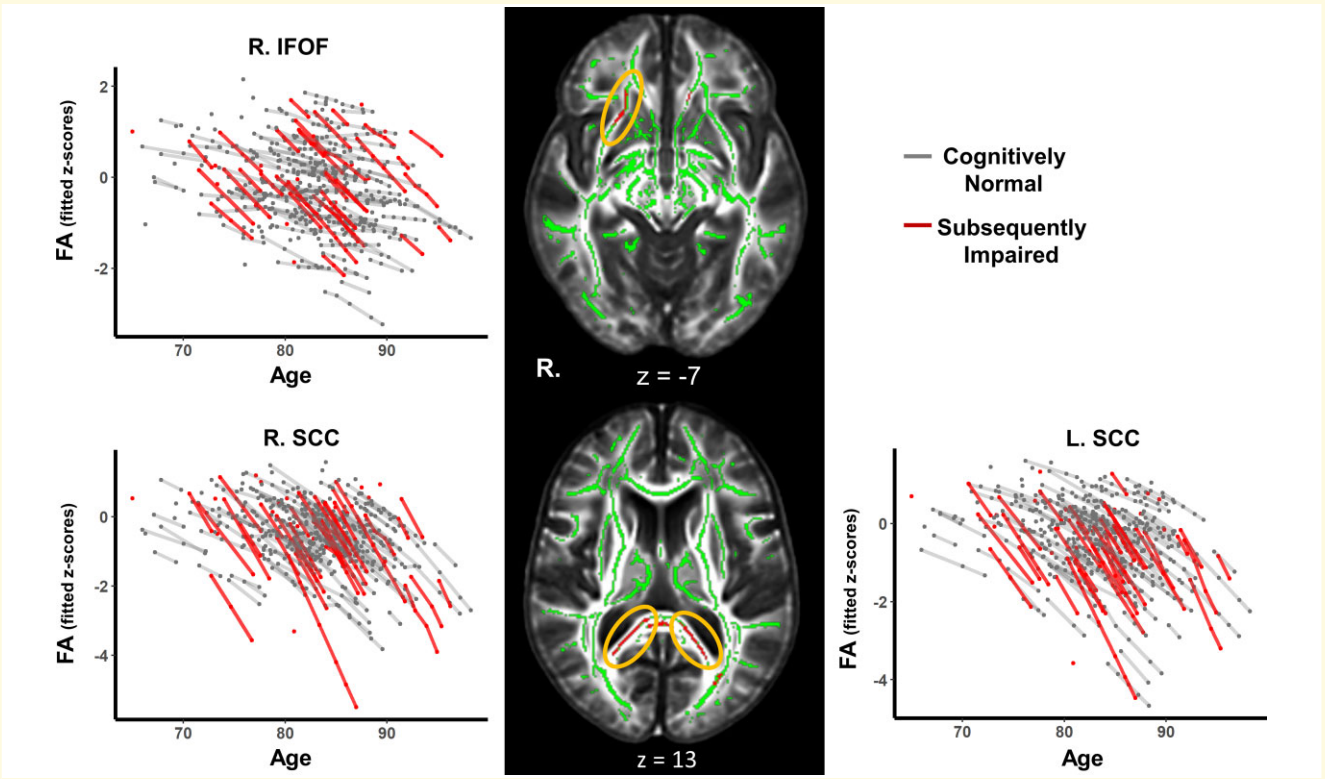

Figure 1 White matter clusters showing accelerated microstructural decline in the SI group. Line graphs show modelled trajectories of a decline in FA for clusters in the right IFOF, right SCC and left SCC. The black panel shows axial slices where clusters with accelerated FA decline were found for the SI group in the right IFOF (*top*) and bilateral SCC (*bottom*) highlighted in red and indicated by the yellow ellipsoids.

Table 3 Differences between SI and CN groups in longitudinal rates of change in cognition and the three main FA clusters showing group differences

Cognitive domain	Beta	*P*-value	Effect size
Verbal memory	**−0.075***	**0.044**	24.93
Executive function	**−0.081***	**0.039**	18.53
Attention	−0.059	0.079	7.21
Verbal fluency	−0.056	0.079	11.06
Visuospatial ability	−0.02	0.530	−11.06
Processing speed	**−0.119****	**<0.001**	41.73
MMSE	−0.099	0.096	18.86
WM ROI[a]	**Beta**	***P*-value**	
Right SCC	**−0.284**	**<0.001**	84
Left SCC	**−0.254**	**<0.001**	75.59
Right IFOF	**−0.175**	**<0.001**	60.78

The linear mixed-effects model controlled for inter-individual differences in age, sex and race. The results reported below for the FA clusters were derived from z-scored, baseline anchored mean raw FA values extracted from the clusters. Here, the models are identical for the cognitive and FA data (see the '*Effect size calculations*' section in Supplementary material). Effect size for differences in longitudinal trajectories between SI and CN groups was determined using a R^2 statistic for multilevel models in which the residual variance in between-person slopes captured by including the effect of subsequent impairment was estimated. MMSE, mini-mental state examination; SCC, splenium of corpus callosum; IFOF, Inferior fronto-occipital fasciculus; SI, subsequently impaired; CN cognitively normal.

[a]All datapoints (subjects and visits) were utilized for the WM ROIs; however, similar results were obtained in analyses based on matched sample sizes between models. Analysis $n = 250$.

* and bold values indicate $P \leq 0.05$.

**Cognitive comparisons that survive FDR correction at $P \leq 0.05$.

longitudinal trajectories of the cognitive measures. Within the cognitive domains examined, longitudinal trajectories for processing speed (42%) and memory (25%) were the most sensitive to subsequent cognitive status, see Table 3.

For the three cognitive domains that showed significantly a faster decline in SI participants (processing speed, memory and executive function), decline in processing speed was associated with decline in FA across all three regions showing faster FA decline in the SI group (L. SCC, $\rho = 0.169$, $P = 0.034$, FDRp = 0.117; R. SCC, $\rho = 0.180$, $P = 0.023$, FDRp = 0.058; R. IFOF, $\rho = 0.265$, $P = 0.001$, FDRp = 0.018; see Fig. 2, left panel). Decline in episodic memory was associated with FA decline in the right IFOF ($\rho = 0.182$, $P = 0.020$, FDRp = 0.037, see Fig. 2, middle panel), whereas no associations were found between decline in executive function and FA in the clusters examined, see Table 4. Of the cognitive domains and MMSE that did not show significantly faster decline for SI participants, decline in MMSE was linked to decline in FA in all clusters, see Fig. 2, right panel, and Table 4. Decline in verbal fluency was associated with FA decline in bilateral SCC, and decline in visuospatial ability with FA decline in the R. IFOF.

Discussion

Using a case–control subset of the BLSA, we found that faster rates of WM microstructural degeneration are detectable before clinical symptoms of MCI or dementia are apparent. Longitudinal voxel-wise analyses identified several clusters (bilateral SCC and right IFOF) where FA declined faster in a sample of SI individuals compared with a control group who remained CN. While several overlapping clusters were found where MD was increasing faster in the SI group compared with controls, these clusters did not remain significant after FDR correction. Furthermore, rates of decline in WM microstructure were associated with rates of decline in cognition in domains that did and did not show significant differences in rates of decline across groups.

The largest clusters to show a faster decline in FA in the SI compared with CN group, and survive FDR correction, were in the left and right SCC. This bilateral pattern of accelerated change indicates that the splenium is susceptible to increased microstructural decline in individuals on a trajectory towards MCI/dementia. Our results extend prior reports of atrophy and reduced microstructure of the SCC in MCI/dementia compared with CN participants[48] and in at risk APOE e4 carriers who show a faster decline in FA in this area.[33] Here we have shown that such changes can be detected in the preclinical stages before the onset of clinical symptoms. The third largest cluster was in the IFOF. The microstructure of the IFOF has been shown to decline faster in Alzheimer's disease patients compared with CN controls[18] and show cross-sectional differences in DTI metrics between preclinical early-onset Alzheimer's disease (EOAD) participants and controls.[49] The SCC contains commissural fibres that connect association regions in the temporal and parietal lobes, including the precuneus,[50] while the IFOF contains fibres connecting frontal and occipital lobes. Evidence suggests that the precuneus and frontal lobe areas are among the earliest regions to accumulate Aβ.[51] Therefore, it is possible that microstructural decline is related to pathological changes occurring in these regions during the preclinical stage of dementia.

Although there were no group differences at baseline in the amount of total WMH volume, a follow-up analysis looking at group differences over time identified a significant interaction (see Supplementary Table 4). WMH volume increased over time in both groups, but the rate of accumulation was faster in SI individuals. FA is lower in areas of WMH, and it has long been known that these two metrics are related. However, DTI is a more sensitive measure than FLAIR for WM damage.[52] Interestingly, WM damage in the SCC, characterized by WM hyperintensities, has been associated with Alzheimer's disease pathology[53,54] and cognition in Alzheimer's disease.[55] Our results add longitudinal evidence to this growing literature highlighting the important effects of dementia on the SCC.

We found no evidence of the faster microstructural decline in limbic structures, including the fornix. This contrasts with Cremers *et al.*[20] who reported that lower baseline FA in limbic tracts was related to an increased risk of dementia and Ringman *et al.*[49] who found cross-sectional evidence of lower FA in the fornix when comparing preclinical EOAD to non-gene carrier family members. These differences may be

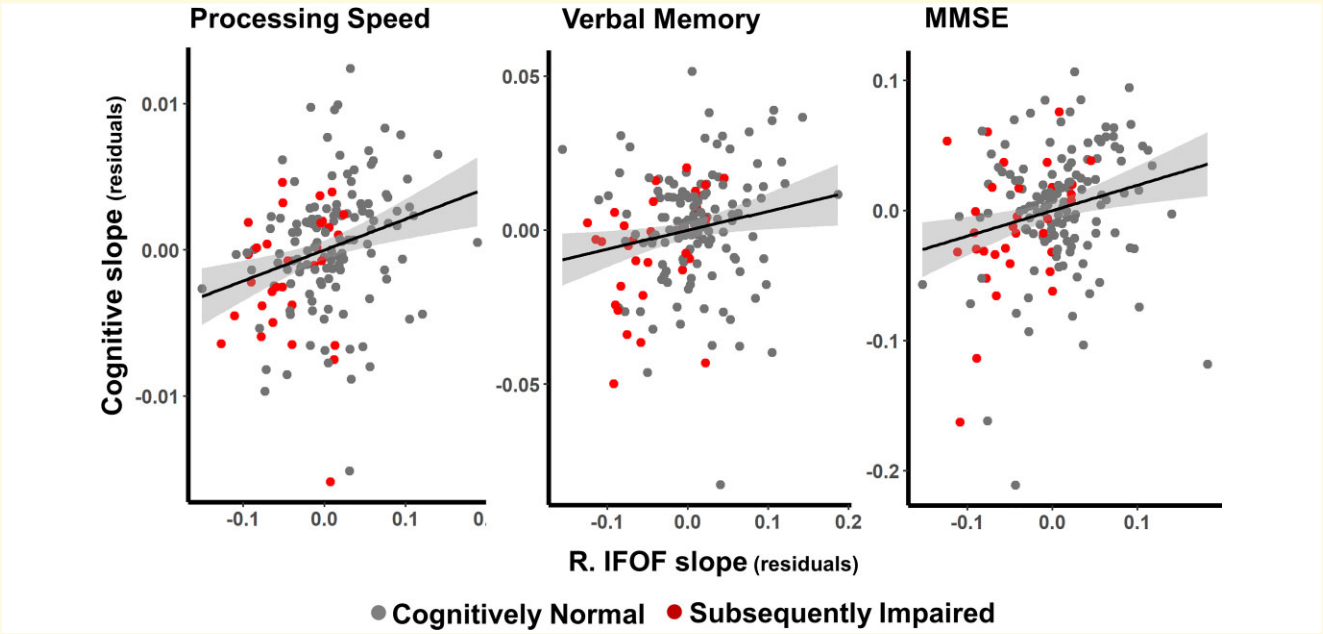

Figure 2 Associations between change in FA and change in cognition. The figure shows the relationship between the rate of change in the right IFOF and the rate of change in processing speed (left panel), verbal memory (middle panel) and MMSE (right panel). The effects of baseline age, sex and race were removed from the estimated slopes for FA and cognition. Thus, the residuals are the estimated slopes of annual change in z-scores removing effects of baseline age, sex, and race. Shaded areas indicate 95% confidence intervals.

Table 4 Associations between change in FA and change in cognition

	Left splenium CC			Right splenium CC			Right IFOF		
	Pearson's *r*	*P*-value	95% CI	Pearson's *r*	*P*-value	95% CI	Pearson's *r*	*P*-value	95% CI
VM	0.106	0.183	−0.05,0.26	0.126	0.111	−0.03,0.28	**0.182**	**0.021****	**0.03,0.33**
EF	0.043	0.606	−0.12,0.19	−0.038	0.649	−0.2,0.11	0.045	0.590	−0.12,0.2
ATT	−0.002	0.98	−0.16,0.15	0.01	0.87	−0.14,0.17	−0.05	0.52	−0.2,0.1
VF	**0.19**	**0.02***	**0.04,0.33**	**0.23**	**0.003****	**0.08,0.37**	0.05	0.52	−0.1,0.2
VSA	0.069	0.386	−0.09,0.22	−0.01	0.9	−0.16,0.15	**0.184**	**0.019****	**0.03,0.33**
PS	**0.167**	**0.038***	**0.01,0.32**	**0.179**	**0.025***	**0.03,0.33**	**0.266**	**0.005****	**0.11,0.4**
MMSE	**0.16**	**0.05***	**0.003,0.3**	**0.185**	**0.02***	**0.03,0.33**	**0.23**	**0.004****	**0.08,0.37**

Associations were determined by partial correlations controlling for age, sex and race. Partial correlations were performed between slopes for subjects with longitudinal data ($n = 168$). Slopes for the FA clusters were derived from applying the simple linear mixed-effects model to z-scored, baseline anchored mean raw FA values extracted from the clusters of interest. VM, verbal memory; EF, executive function; ATT, attention; VF, verbal fluency; VSA, visuospatial ability; PS, processing speed; SCC, splenium of corpus callosum; IFOF, inferior fronto-occipital fasciculus.

* and bold values indicate $P \leq 0.05$.

**Survives FDR correction at $P \leq 0.05$.

due to methodological differences as both previous studies employed ROIs rather than a TBSS approach. Another cross-sectional study of preclinical EOAD participants compared with CN controls used TBSS and found no difference in DTI metrics in the fornix.[56]

Cognitively characterizing this DTI subsample of the BLSA confirmed that the SI group had similar preclinical cognitive profiles to other preclinical samples.[14,57] Cognitive trajectories for three domains (verbal memory, executive function and processing speed) showed a faster decline in SI individuals. The pattern for all cognitive outcomes examined, apart from visuospatial ability, was similar with trends towards a greater decline in the SI group. The exception of visuospatial ability is interesting as our recent publication of change-points in Alzheimer's disease in a larger BLSA preclinical sample with subsequent probable Alzheimer's disease found the earliest change-point in cognition for these participants was visuospatial ability.[15] There are three main differences between the current sample and the one used in the change-point analysis that shed light on why these results differ. The first is time to diagnosis. Here we were restricted to data from visits that also contained diffusion-weighted imaging. The BLSA collected cognitive measures well before the collection of diffusion-weighted images and as such the time to diagnosis from the first visit with DTI data in the present sample is considerably shorter {from 10 years [6.5 standard deviation (SD)] in Williams *et al.*[15] to 4 years (1.9 SD) here}. This also shifts baseline

age in the current sample to an older mean age. Second, and related to the first difference, is the smaller number of BLSA participants with diffusion-weighted data that went on to develop cognitive impairment ($n = 165$ in Williams *et al.*[15] versus $n = 50$ here). Finally, the inclusion of individuals with MCI and all-cause dementia in the present study was necessary to increase the sample size due to the more recent introduction of DTI. Therefore, there was increased heterogeneity in cognitive trajectories in the SI sample due to the inclusion of both MCI and dementia end-points. These findings and considerations suggest that the present sample has either missed the 'window' for group differences in visuospatial ability or obscured differences in this cognitive domain due to the inclusion of different types of dementia.

Comparing the effect size (R^2) for group membership (proportion of explained variance in rates of change by group membership), we found FA to yield considerably higher values compared with the cognitive outcomes. These findings are not surprising as the cognitive data are more variable over time due to a greater number of factors influencing performance. However, these findings suggest that regional changes over time in DTI markers may provide a more robust marker of changes during preclinical dementia.

Associations between change in FA and change in cognition were observed for five cognitive domains. Of the three domains that showed significant differences in decline by group, a faster decline in FA in the R IFOF was associated with the faster decline in verbal memory, and a faster decline in FA in all three clusters was related to a faster decline in processing speed. In addition, faster FA decline in all three clusters was related to MMSE, while the splenium clusters were linked to declines in verbal fluency and the R IFOF to visuospatial ability. These results extend previous findings in which regional differences in frontal lobe WM microstructure between Alzheimer's disease and controls were also correlated with memory performance.[57] While splenium FA decline was not related to verbal memory, it was related to verbal fluency, processing speed and MMSE. These results are consistent with a previous cross-sectional report showing FA in the splenium is associated with poorer cognition in MCI/dementia patients as measured by the CDR scale.[58] The finding that processing speed was related to FA decline in all three clusters is perhaps less surprising given previous reports of significant associations between WM microstructure in these areas and processing speed in CN older adults.[59]

Results from this study should be considered in the context of several limitations. BLSA participants in this sample are highly educated, mostly white and relatively old, with a mean baseline age of 80 years, which may limit generalizability. Furthermore, the follow-up period was relatively short, and while most participants had multiple DTI and cognitive assessments, some only contributed cross-sectional data. Longitudinal data collection requires a balance between the need to maintain consistent imaging parameters and updating acquisition methods to allow comparisons over time. As a result, the standard DTI acquisitions in the BLSA have been held constant since the introduction of DTI into the BLSA 3 T MRI imaging protocol. It is possible that more modern diffusion imaging sequences would be more sensitive to changes in WM structure related to changes in early preclinical stages of dementia. However, the sample size and longitudinal power are still improvements in previous studies of preclinical changes in DTI. The SI sample included participants, who were CN at the time of imaging but had research diagnoses of either MCI or dementia as their final cognitive status at the time of analysis. While MCI is typically the prodromal stage of Alzheimer's disease,[60] it is possible that some MCI participants will remain stable or develop non-Alzheimer's disease pathologies. This heterogeneity may increase variance in the SI group, leading to an underestimation of the extent of localized WM microstructural damage in preclinical dementia. Unfortunately, there were not enough participants in the sample who also had amyloid imaging to examine the role of Alzheimer's disease pathology on WM microstructural damage, this should be addressed in future works with larger sample sizes and the availability of new plasma biomarkers. Moreover, future work with larger samples of all-cause dementia and Alzheimer's disease cases separately may address this issue. The study benefits from the statistical matching of SI to CN participants with similar demographic features, allowing for higher confidence that the differences found between groups are indeed a result of the group differences in disease trajectories. However, we cannot exclude the possibility that some individuals in the CN group will develop cognitive impairment later, and it is possible that more robust differences may be found in samples where the cause of dementia and Alzheimer's disease pathology is confirmed post-mortem.

In this study, longitudinal DTI data were used to characterize voxel-wise patterns of accelerated decline in WM microstructure and its relationship to cognition during the preclinical phase of MCI/dementia. Group membership explained more variance in rates of change in regional brain microstructure than it did in cognitive decline, suggesting DTI may be a powerful indicator of future risk of developing MCI/dementia. To find the optimal imaging markers of preclinical dementia, future work should focus on elucidating the joint associations and temporal relationships between change in regional DTI metrics and changes in other markers of dementia such as atrophy and Aβ accumulation in the preclinical stage of Alzheimer's disease.

Acknowledgements

We thank the staff of the BLSA and the National Institute on Aging 3 T MRI facility for their assistance and the BLSA participants for their dedication to this study.

Funding

This research was supported by the Intramural Research Program of the National Institutes of Health, National Institute on Aging.

Competing interest

The authors report no competing interests.

Supplementary material

Supplementary material is available at *Brain Communications* online.

References

1. Nitrini R, Bottino CMC, Albala C, *et al.* Prevalence of dementia in Latin America: A collaborative study of population-based cohorts. *Int Psychogeriatr*. 2009;21(4):622–630.
2. Armstrong NM, Huang C-W, Williams OA, *et al.* Sex differences in the association between amyloid and longitudinal brain volume change in cognitively normal older adults. *NeuroImage*. 2019;22:101769.
3. Jack CR Jr, Bennett DA, Blennow K, *et al.* NIA-AA Research Framework: Toward a biological definition of Alzheimer's disease. *Alzheimers Dement*. 2018;14(4):535–562.
4. Sperling RA, Aisen PS, Beckett LA, *et al.* Toward defining the preclinical stages of Alzheimer's disease: Recommendations from the National Institute on Aging-Alzheimer's Association workgroups on diagnostic guidelines for Alzheimer's disease. *Alzheimers Dement*. 2011;7(3):280–292.
5. Villemagne VL, Burnham S, Bourgeat P, *et al.* Amyloid β deposition, neurodegeneration, and cognitive decline in sporadic Alzheimer's disease: A prospective cohort study. *Lancet Neurol*. 2013;12(4):357–367.
6. Damoiseaux JS, Prater KE, Miller BL, *et al.* Functional connectivity tracks clinical deterioration in Alzheimer's disease. *Neurobiol Aging*. 2012;33(4):828.e19–28.e30.
7. Jones DT, Knopman DS, Gunter JL, *et al.* Cascading network failure across the Alzheimer's disease spectrum. *Brain*. 2016;139(2):547–562.
8. Basser PJ, Mattiello J, LeBihan D. MR diffusion tensor spectroscopy and imaging. *Biophys J*. 1994;66(1):259–267.
9. Barrick TR, Charlton RA, Clark CA, Markus HS. White matter structural decline in normal ageing: A prospective longitudinal study using tract-based spatial statistics. *Neuroimage*. 2010;51(2):565–577.
10. Charlton RA, Schiavone F, Barrick TR, Morris RG, Markus HS. Diffusion tensor imaging detects age related white matter change over a 2 year follow-up which is associated with working memory decline. *J Neurol Neurosurg Psychiatry*. 2010;81(1):13–19.
11. Kennedy KM, Raz N. Aging white matter and cognition: Differential effects of regional variations in diffusion properties on memory, executive functions, and speed. *Neuropsychologia*. 2009;47(3):916–927.
12. Salat DH, Tuch DS, Greve DN, *et al.* Age-related alterations in white matter microstructure measured by diffusion tensor imaging. *Neurobiol Aging*. 2005;26(8):1215–1227.
13. Sexton CE, Walhovd KB, Storsve AB, *et al.* Accelerated changes in white matter microstructure during aging: A longitudinal diffusion tensor imaging study. *J Neurosci*. 2014;34(46):15425–15436.
14. Bäckman L, Jones S, Berger A-K, Laukka EJ, Small BJ. Cognitive impairment in preclinical Alzheimer's disease: A meta-analysis. *Neuropsychology*. 2005;19(4):520–531.
15. Williams OA, An Y, Armstrong NM, Kitner-Triolo M, Ferrucci L, Resnick SM. Profiles of cognitive change in preclinical and prodromal Alzheimer's disease using change-point analysis. *J Alzheimers Dis*. 2020;75:1169–1180.
16. Alm KH, Bakker A. Relationships between diffusion tensor imaging and cerebrospinal fluid metrics in early stages of the Alzheimer's disease continuum. *J Alzheimers Dis*. 2019;70:965–981.
17. Clerx L, Visser PJ, Verhey F, Aalten P. New MRI markers for Alzheimer's disease: A meta-analysis of diffusion tensor imaging and a comparison with medial temporal lobe measurements. *J Alzheimers Dis*. 2012;29:405–429.
18. Kitamura S, Kiuchi K, Taoka T, *et al.* Longitudinal white matter changes in Alzheimer's disease: A tractography-based analysis study. *Brain Res*. 2013;1515:12–18.
19. Sexton CE, Kalu UG, Filippini N, Mackay CE, Ebmeier KP. A meta-analysis of diffusion tensor imaging in mild cognitive impairment and Alzheimer's disease. *Neurobiol Aging*. 2011;32(12):2322.e5–2322.e18.
20. Cremers LGM, Wolters FJ, de Groot M, *et al.* Structural disconnectivity and the risk of dementia in the general population. *Neurology*. 2020;95(11):e1528–e1537.
21. Sevigny J, Chiao P, Bussière T, *et al.* The antibody aducanumab reduces Aβ plaques in Alzheimer's disease. *Nature*. 2016;537(7618):50–56.
22. Sperling RA, Rentz DM, Johnson KA, *et al.* The A4 study: Stopping AD before symptoms begin? *Sci Transl Med*. 2014;6(228):228fs13–228fs13.
23. Shock NW. *Normal human aging: The Baltimore longitudinal study of aging*. 1984.
24. Ho DE, Imai K, King G, Stuart EA. Matching as nonparametric preprocessing for reducing model dependence in parametric causal inference. *Pol Anal*. 2007;15(3):199–236.
25. Resnick SM, Pham DL, Kraut MA, Zonderman AB, Davatzikos C. Longitudinal magnetic resonance imaging studies of older adults: A shrinking brain. *J Neurosci*. 2003;23(8):3295–3301.
26. Morris JC. The Clinical Dementia Rating (CDR): Current version and scoring rules. *Neurology*. 1993;43:2412–2414.
27. Fuld PA. Psychological testing in the differential diagnosis of the dementias. *Alzheimer Dis*. 1978;7:185–193.
28. Association AP. *Diagnostic and statistical manual of mental health disorders (DSM-III-R)*. American Psychiatric Association; 1987.
29. McKhann G, Drachman D, Folstein M, Katzman R, Price D, Stadlan EM. Clinical diagnosis of Alzheimer's disease Report of the NINCDS-ADRDA Work Group* under the auspices of Department of Health and Human Services Task Force on Alzheimer's Disease. *Neurology*. 1984;34(7):939–939.
30. Petersen RC, Smith GE, Waring SC, Ivnik RJ, Tangalos EG, Kokmen E. Mild cognitive impairment: Clinical characterization and outcome. *Arch Neurol*. 1999;56:303–308.
31. Lauzon CB, Asman AJ, Esparza ML, *et al.* Simultaneous analysis and quality assurance for diffusion tensor imaging. *PLoS One*. 2013;8(4):e61737.
32. Venkatraman VK, Gonzalez CE, Landman B, *et al.* Region of interest correction factors improve reliability of diffusion imaging measures within and across scanners and field strengths. *NeuroImage*. 2015;119:406–416.
33. Williams OA, An Y, Beason-Held L, *et al.* Vascular burden and APOE ϵ4 are associated with white matter microstructural decline in cognitively normal older adults. *NeuroImage*. 2019;188:572–583.
34. Smith SM, Jenkinson M, Johansen-Berg H, *et al.* Tract-based spatial statistics: Voxelwise analysis of multi-subject diffusion data. *Neuroimage*. 2006;31(4):1487–1505.
35. Avants BB, Tustison NJ, Song G, Cook PA, Klein A, Gee JC. A reproducible evaluation of ANTs similarity metric performance in brain image registration. *Neuroimage*. 2011;54(3):2033–2044.
36. Doshi J, Erus G, Ou Y, *et al.* MUSE: MUlti-atlas region Segmentation utilizing Ensembles of registration algorithms and parameters, and locally optimal atlas selection. *Neuroimage*. 2016;127:186–915.
37. Doshi J, Erus G, Habes M, Davatzikos C. DeepMRSeg: A convolutional deep neural network for anatomy and abnormality segmentation on MR images. arXiv preprint arXiv:190702110 2019.

38. McCarrey AC, An Y, Kitner-Triolo MH, Ferrucci L., Resnick SM. Sex differences in cognitive trajectories in clinically normal older adults. *Psychol Aging*. 2016;31(2):166–175.
39. Pezzotti P, Scalmana S, Mastromattei A, Di Lallo D. The accuracy of the MMSE in detecting cognitive impairment when administered by general practitioners: A prospective observational study. *BMC Fam Pract*. 2008;9(1):29.
40. Armstrong NM, An Y, Shin JJ, *et al.* Associations between cognitive and brain volume changes in cognitively normal older adults. *Neuroimage*. 2020;223:117289.
41. Shafer AT, Beason-Held L, An Y, *et al.* Default mode network connectivity and cognition in the aging brain: The effects of age, sex, and APOE genotype. *Neurobiol Aging*. 2021;104:10–23.
42. Williams OA, An Y, Armstrong NM, *et al.* Apolipoprotein E ϵ4 allele effects on longitudinal cognitive trajectories are sex and age dependent. *Alzheimers Dement*. 2019;15(12):1558–1567. [published Online First: 2019/09/29].
43. Genovese CR, Lazar NA, Nichols T. Thresholding of statistical maps in functional neuroimaging using the false discovery rate. *Neuroimage*. 2002;15(4):870–878.
44. Mori S, Oishi K, Jiang H, *et al.* Stereotaxic white matter atlas based on diffusion tensor imaging in an ICBM template. *Neuroimage*. 2008;40(2):570–582.
45. Lorah J. Effect size measures for multilevel models: Definition, interpretation, and TIMSS example. *Large-Scale Assess Educ*. 2018;6(1):8.
46. Singer JD, Willett JB, Willett JB. *Applied longitudinal data analysis: Modeling change and event occurrence*. Oxford University Press; 2003.
47. Kim S. ppcor: An R package for a fast calculation to semi-partial correlation coefficients. *Commun Stat Appl Methods*. 2015;22(6):665–674.
48. Di Paola M, Spalletta G, Caltagirone C. In vivo structural neuroanatomy of corpus callosum in Alzheimer's disease and mild cognitive impairment using different MRI techniques: A review. *J Alzheimers Dis*. 2010;20(1):67–95.
49. Ringman JM, O'Neill J, Geschwind D, *et al.* Diffusion tensor imaging in preclinical and presymptomatic carriers of familial Alzheimer's disease mutations. *Brain*. 2007;130(7):1767–1776.
50. Hofer S, Frahm J. Topography of the human corpus callosum revisited—Comprehensive fiber tractography using diffusion tensor magnetic resonance imaging. *NeuroImage*. 2006;32(3):989–994.
51. Bilgel M, Prince JL, Wong DF, Resnick SM, Jedynak BM. A multivariate nonlinear mixed effects model for longitudinal image analysis: Application to amyloid imaging. *NeuroImage*. 2016;134:658–670.
52. O'Sullivan M, Summers PE, Jones DK, Jarosz JM, Williams SCR, Markus HS. Normal-appearing white matter in ischemic leukoaraiosis: A diffusion tensor MRI study. *Neurology*. 2001;57(12):2307–2310.
53. Garnier-Crussard A, Bougacha S, Wirth M, *et al.* White matter hyperintensity topography in Alzheimer's disease and links to cognition. *Alzheimers Dement*. 2021. Advance Access published on July 28, 2021, doi: 10.1002/alz.12410.
54. Gaubert M, Lange C, Garnier-Crussard A, *et al.* Topographic patterns of white matter hyperintensities are associated with multimodal neuroimaging biomarkers of Alzheimer's disease. *Alzheimers Res Ther*. 2021;13:29.
55. Weaver NA, Doeven T, Barkhof F, *et al.* Cerebral amyloid burden is associated with white matter hyperintensity location in specific posterior white matter regions. *Neurobiol Aging*. 2019;84:225–234.
56. Li X, Westman E, Ståhlbom A, *et al.* White matter changes in familial Alzheimer's disease. *J Intern Med*. 2015;278(2):211–218.
57. Huang J, Auchus AP. Diffusion tensor imaging of normal appearing white matter and its correlation with cognitive functioning in mild cognitive impairment and Alzheimer's disease. *Ann N Y Acad Sci*. 2007;1097(1):259–264.
58. Mielke MM, Kozauer NA, Chan KCG, *et al.* Regionally-specific diffusion tensor imaging in mild cognitive impairment and Alzheimer's disease. *Neuroimage*. 2009;46(1):47–55.
59. Kerchner GA, Racine CA, Hale S, *et al.* Cognitive processing speed in older adults: Relationship with white matter integrity. *PLoS One*. 2012;7(11):e50425.
60. Jack CR Jr, Albert MS, Knopman DS, *et al.* Introduction to the recommendations from the National Institute on Aging–Alzheimer's Association workgroups on diagnostic guidelines for Alzheimer's disease. *Alzheimers Dement*. 2011;7(3):257–262.